Electrospray Ionization Fourier Transform Mass Spectrometric Analysis of Wine

Helen J. Cooper and Alan G. Marshall*

Center for Interdisciplinary Magnetic Resonance, National High Magnetic Field Laboratory, Florida State University, 1800 East Paul Dirac Drive, Tallahassee, Florida 32310

Positive- and negative-ion electrospray ionization Fourier transform ion cyclotron resonance (FT-ICR) mass spectrometry has been used for direct analysis of five wines (California Red, Corbiere, Zinfandel, Beaujolais, and Sauvignon Blanc), without any prior separation or purification steps. The high mass resolving power (typically $m/\Delta m_{50\%} \geq 80000$, in which $\Delta m_{50\%}$ is mass spectral peak full width at half-maximum peak height) and mass accuracy (≤1 ppm) of FT-ICR mass spectrometry make it ideal for the study of complex mixtures such as wine, because the components are simultaneously resolved and identified as to elemental composition. Moreover, the high dynamic range of the instrument is advantageous for identifying trace components. The positive-ion mass spectra obtained from the wines were somewhat similar and were dominated by sucrose and (for red wines) anthocyanins. More than 30 compounds (phenolics and carbohydrates) were identified. The negative-ion mass spectra exhibited much greater variation among different wines, with several compounds peculiar to each wine. Elemental compositions could be assigned with high confidence to 76−94% of negative ions of >10% relative abundance. The present results suggest that it may be possible to fingerprint a wine on the basis of its negative-ion ESI FT-ICR mass spectrum.

Keywords: *FTMS; FT-ICR; FTICR; mass spectrometry; electrospray ionization; ESI; exact mass; accurate mass; elemental composition; chemical formula; wine classification*

INTRODUCTION

An understanding of the composition of wine is important for many reasons. For example, analysis of the phenolic compounds in wine is of great interest due to their organoleptic (i.e., those perceived by a sense organ) properties. Anthocyanins are responsible for the color of red wine (*1*) and condensed tannins for astringency (*2*). The phenolic compounds also possess antibacterial and antioxidant properties believed to be responsible for the "French paradox", namely, increased protection from heart disease in consumers. The peptides in wine also influence its characteristics. Sulfur-containing compounds affect wine aroma (*3*), as do terpenoids and norisoprenoid derivatives (*4*). It would also be of interest, particularly to the wine industry and regulatory bodies, to be able to determine the varietal origin of grapes and wines from their chemical compositions.

Traditionally, the analysis of wine has relied heavily on extraction and separation of the compounds of interest, due to its chemical complexity. Many studies have concentrated on the phenolic fingerprint, in particular, the anthocyanin profile. The anthocyanin profile is distinctive to each plant species and is used in chemotaxonomy and verification of authenticity in food products (*5*). Prior to analysis, the anthocyanins are extracted from plants or wine. The crude anthocyanin extracts are initially purified by solid phase extraction (SPE) (*6*). Traditionally, separation of the anthocyanins was achieved by reversed-phase high-performance liquid chromatography (HPLC) coupled with UV diode array detection, allowing for on-line collection of the spectra (*7*−*11*). UV−vis absorbance spectra of anthocyanins provide information on the aglycon, the glycosylation pattern, and the possibility of acylation.

More recently, liquid chromatography−mass spectrometry (LC-MS) techniques have been applied to the analysis of anthocyanins. Glässgen et al. (*12*) used liquid chromatography electrospray ionization mass spectrometry (LC-ESI-MS) to identify anthocyanins in Indian black carrot. Several groups have used HPLC combined with electrospray ionization (*13*−*15*) to study anthocyanins present in grape and wine extracts (*7*, *16*−*20*). Wang and Sporns (*21*) used matrix-assisted laser desorption/ionization (MALDI) mass spectrometry to analyze anthocyanins in red wines and fruit juices, with prior extraction of the anthocyanins.

Other techniques have been considered for wine classification. Recently, Edelmann et al. (*22*) found that mid-infrared spectroscopy of phenolic extracts of wine could be used to discriminate between cultivars. The same was not true of untreated wines due to interference from other components including sugars and organic acids. Siret et al. (*23*) considered the residual DNA in must and wine as a classification method but found the low concentration to be a limiting factor.

The presence and relative abundances of many other components of wine depend on both the grape variety and the wine-making process. Although peptides exhibit surfactant and organoleptic properties, few studies of peptide composition have been conducted (*24*, *25*) due to the difficulty in their isolation. Moreno-Arribas et al. (*25*) and Desportes et al. (*24*) have developed methods for peptide isolation and analysis. Similarly, monophosphate nucleotides are difficult to identify in wine due

* Address correspondence to this author at the Department of Chemistry, Florida State University, Tallahassee, FL 32310.

10.1021/jf0108516 CCC: $20.00
Published on Web 11/03/2001

to its complexity. Recently, Aussenac et al. (*26*) developed a method for isolating and purifying those compounds from Champagne wine and analyzed them by HPLC-ESI mass spectrometry.

The extraction and separation techniques used in the analysis of wine components are time-consuming, are not exhaustive, and can result in artifacts (*27*). Moreover, the consumer qualities of wine (flavor and aroma) are not due to single components. The varietal origin alone does not determine a wine's final state. To classify a wine, one needs to consider the entire mixture. Here, we introduce electrospray ionization combined with Fourier transform ion cyclotron resonance (FT-ICR) (*28*, *29*) mass spectrometry to characterize wines *without* prior extraction or separation. FT-ICR MS routinely provides mass resolving power, $m/\Delta m_{50\%} > 80000$ (in which m is ion mass and $\Delta m_{50\%}$ denotes mass spectral peak full width at half-maximum height), and mass accuracy better than 1 ppm. These high specifications mean that FT-ICR is ideal for analyzing complex mixtures, as demonstrated by prior ESI FT-ICR MS analysis of petroleum crude oils containing thousands of chemically distinct constituents (*30*, *31*). Moreover, it becomes possible to assign molecular formulas ($C_cH_hN_nO_oS_s$) unambiguously by mass measurement alone for singly charged ions up to ~450 Da. Our present home-built instrument (*32*, *33*) offers high magnetic field (9.4 T) for high mass resolution and mass accuracy (*34*) and a large (about twice the diameter of a commercial instrument) FT-ICR trapped-ion cell for high dynamic range. Resolution and detection of trace components is therefore improved. Because ESI FT-ICR MS eliminates the need for prior chromatographic separation, the possibility of chemical modifications during analysis is minimized.

We have acquired both positive-ion and negative-ion ESI FT-ICR mass spectra of five wines. Approximately 30 known components were identified in the positive-ion mass spectra. The negative-ion mass spectra showed far greater variation in the nature and relative abundances of different chemical components among the wines. Positive-ion ESI results in the attachment of sodium and potassium cations and protons, whereas negative-ion ESI produces deprotonation, allowing simpler assignment of molecular formula (elemental composition). We are able to assign unique elemental compositions to 76−94% of the negative ions of >10% relative abundance. No species observed as protonated ions in the positive ESI spectra were observed as deprotonated ions in the negative ESI spectra, presumably because compounds observed by positive electrospray are basic, whereas compounds observed in negative electrospray are acidic.

EXPERIMENTAL METHODS

Samples. Five wines were studied: Inglenook California Chianti (henceforth denoted California Red to distinguish it from genuine Chianti), Chorus Red Corbiere (1998), Rancho Zabaco California Red Zinfandel (unfiltered) (1997), Cuvee Plateau de Bel-Air, Brouilly Red Beaujolais (1999), and Corbett Canyon Chilean Sauvignon Blanc. All were purchased from local markets in Tallahassee, FL. Electrospray ionization reagents were purchased from J. T. Baker (Philipsburg, NJ) and used without further treatment.

Electrospray Sample Preparation. For positive electrospray ionization, 10 μL of wine was diluted with 90 μL of 1:1 methanol/water. It was neither necessary nor desirable to add acid to the samples, due to the significant natural acid content of wine. For negative electrospray ionization, 10 μL of wine was diluted with 90 μL of 1:1 methanol/5 mM ammonium acetate. No extraction or purification was performed. Background spectra of the electrospray matrix (1:1 methanol/water) were run prior to each analysis. No ions were observed. The wine spectra therefore wholly reflect components of wine and not solvent cluster ions.

Electrospray Ionization High-Field FT-ICR Mass Spectrometry. The wine samples were analyzed with a home-built, passively shielded, 9.4 T FT-ICR mass spectrometer (*32*) equipped with an external microelectrospray ionization source (*33*). The samples were infused at a flow rate of 300 nL/min through an electrospray emitter consisting of a 50 μm i.d. fused silica capillary, which had been mechanically ground to a uniform thin-walled tip (*35*). A potential of 2.0 kV was applied between the microspray emitter and the capillary entrance. The electrosprayed ions were delivered into the mass spectrometer through a Chait-style atmosphere-to-vacuum interface (*36*) and externally accumulated (*33*) for 4 s in a 45 cm radio frequency-only octapole. The ions were transferred through multipole ion guides and trapped in an open (*37*) cylindrical cell. The ions were chirp excited (72−640 kHz at 150 Hz/μs) and detected in direct mode (512 kword time-domain data). Two hundred time-domain data sets were coadded, Hanning apodized, zero-filled once, and subjected to fast Fourier transform (FFT) followed by magnitude calculation. The experimental event sequence was controlled by a modular ICR data acquisition system (MIDAS) (*38*).

Mass Calibration. The FT-ICR mass spectra were internally frequency-to-m/z calibrated (*39*, *40*) with respect to ions of known elemental composition in the wine. For positive-ion ESI, the red wines were calibrated with respect to potassiated sucrose [theoretical $[M + K]^+$ mass, 381.07938 Da), malvidin 3-glucoside (493.13407 Da), and malvidin 3-glucoside *p*-coumarate (639.17085 Da]. The Sauvignon Blanc sample was calibrated with respect to four potassiated carbohydrate ions of theoretical $[M + K]^+$ masses 351.06886, 381.07938, 543.13226, and 645.16386 Da. For negative-ion ESI, the Corbiere sample was calibrated with respect to the deprotonated tartaric acid dimer (theoretical $[M - H]^-$ mass of 299.02560 Da) and two carbohydrate ions of theoretical $[M - H]^-$ mass of 503.16172 and 605.19288 Da. The remaining wine samples did not contain peaks at m/z 503.16172 and were calibrated with respect to the tartaric acid dimer (m/z 299.02560), the carbohydrate ion (m/z 605.19288), and a peak assigned from the Corbiere spectrum as $C_{10}H_{15}O_{13}^-$ (m/z 343.05181) that appeared in all of the negative-ion spectra. All mass measurements are based on the "monoisotopic" ion (i.e., the species in which all carbons are ^{12}C, all oxygens are ^{16}O, all nitrogens are ^{14}N, etc.).

Data Analysis. FT-ICR mass spectral data were analyzed by use of the MIDAS Analysis software package (*41*). Elemental compositions were generated with Masscalc (Softshell International Ltd., Grand Junction, CO). At an average mass resolving power, $m/\Delta m_{50\%} = 66000$ (in which $\Delta m_{50\%}$ is the full mass spectral peak width at half-maximum peak height), the average difference between calculated and experimental masses was ~0.5−1.0 ppm throughout a mass range of 300−700 Da. Moreover, the relative abundances within the isotopic distribution for each of the ionic species provide an independent criterion for the elements to be included in a given molecular formula (e.g., ^{12}C, ^{13}C, H, ^{14}N, ^{16}O, ^{32}S, and ^{34}S) (*42*). The isotopic distributions also reveal the ion's charge state (e.g., the mass spectral peaks for doubly charged $[M + 2H]^{2+}$ ions with no or one ^{13}C atoms will be spaced ~0.5 Da apart, compared to ~1 Da for the corresponding singly charged $[M + H]^+$ ions). In fact, all of the ions observed were singly charged. The elements and errors were entered into the MassCalc package from which possible elemental compositions were generated.

RESULTS AND DISCUSSION

Positive-Ion Electrospray FT-ICR Mass Spectra. Positive-ion ESI FT-ICR mass spectra obtained from the

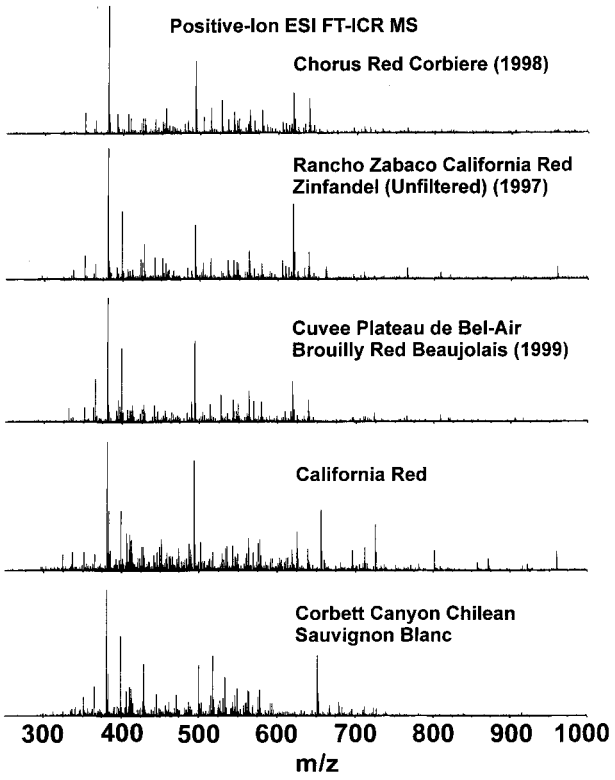

Figure 1. Positive-ion ESI FT-ICR mass spectrum of each of five wines.

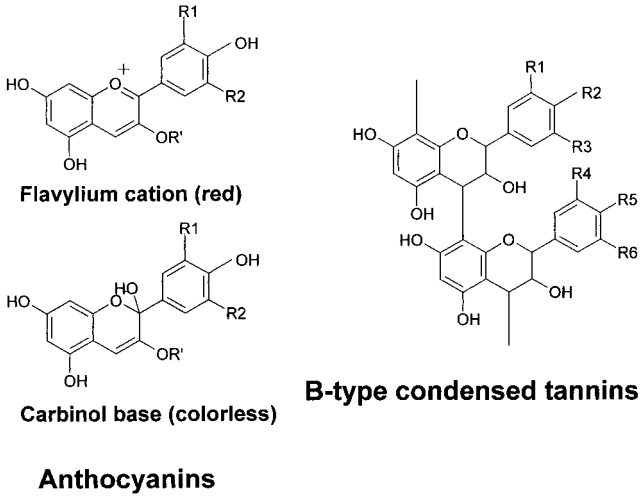

Figure 2. Molecular structures of some phenolic compounds observed in wine.

five wine samples are shown in Figure 1. On the basis of internal calibration, the average root-mean-square (rms) error over the *m*/*z* range 381−640 is 0.51 ppm, indicating that the elemental composition may be assigned uniquely with high confidence.

Phenolics. Structures of various assigned phenolic compounds are shown in Figures 2 and 3. Although the unrivaled mass accuracy of FT-ICR mass spectrometry yields unique elemental compositions for most ions below ~450 Da, additional techniques are needed to assign molecular formulas for species of higher mass. For example, infrared multiphoton dissociation (IRMPD) (*43*, *44*), sustained off-resonance collision-induced dissociation (SORI-CID) (*45*), and (for multiply charged ions) electron capture dissociation (ECD) (*46*) are commonly used. However, even such fragmentation techniques cannot necessarily distinguish between optical isomers. In this paper, structural assignments are based on elemental compositions from accurate mass measurements, combined with knowledge of some known structures of molecules previously identified in wines. On that basis, >30 compounds could be resolved, assigned to unique molecular formulas, and assigned to probable molecular structures.

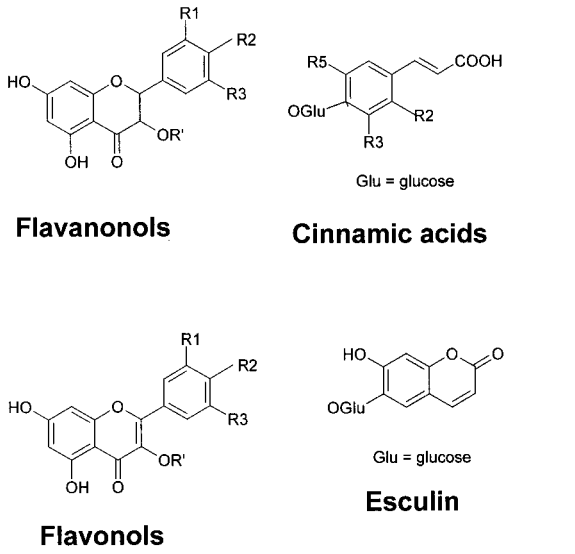

Figure 3. Molecular structures of other phenolic compounds observed in wines.

Anthocyanins. Anthocyanins comprise a flavanoid component, known as an anthocyanidin, conjugated with glucose (see Figure 2; R′ = glucose). In wine, anthocyanins exist in dynamic equilibrium among five major forms including the flavylium cation ($M^{\bullet+}$, responsible for red coloring) and the carbinol (colorless). Peonidin 3-glucoside (R1 = OCH_3; R2 = H; theoretical mass of 463.1235), delphinidin 3-glucoside (R1 = OH; R2 = OH; theoretical mass of 465.1028 Da), petunidin 3-glucoside (R1 = OCH_3; R2 = OH; theoretical mass of 479.1185 Da), and malvidin 3-glucoside (R1 = OCH_3; R2 = OCH_3; theoretical mass of 493.1341 Da) were identified in the flavylium state in the Corbiere, California Red, Zinfandel, and Beaujolais wines. The flavylium ion *p*-coumarates of peonidin 3-glucoside (theoretical mass of 609.1602 Da), petunidin 3-glucoside (theoretical mass of 625.1552 Da), and malvidin 3-glucoside (theoretical mass of 639.1709 Da) were also identified in all four red wines. The protonated carbinol $[M + H]^+$ forms of delphinidin 3-glucoside (theoretical mass of 483.1139 Da) and malvidin 3-glucoside (theoretical mass of 511.1447 Da) were identified in the Corbiere, Beaujolais, and California Red wines. As expected, no anthocyanins were seen in the Sauvignon Blanc (white wine) sample.

Tannins. Condensed tannins (see Figure 2) exist as oligomers and polymers of flavan-3-ols. They are also referred to as proanthocyanidins because their upper units yield the colored anthocyanidins when heated in acidic medium—procyanidins (R1, R2 = OH; R3 = H) resulting in cyanidin cations and prodelphinidins (R1, R2, R3 = OH) resulting in delphinidin cations (*47*−*49*). Previous work has shown the existence of mixed oligomers containing both dihydroxylated and trihydroxylated flavonol units (*49*). Several peaks corresponding to the masses of dimers (as opposed to cation-bound dimers) of B-type condensed tannins were observed in

the positive-ion ESI FT-ICR mass spectra. (Peaks corresponding to the masses of the less common A-type condensed tannins were not observed.) Peaks corresponding to both protonated (theoretical mass of 579.1498 Da) and potassiated (theoretical mass of 617.1057 Da) homodimers of catechin (or epicatechin, its structural isomer) were observed in the positive-ion mass spectra of the Corbiere, Zinfandel, and Beaujolais samples. Only the potassiated homodimer was observed for the California Red sample. For the Corbiere sample, peaks corresponding to the protonated ($[M_1 + M_2 + H]^+$, theoretical mass of 595.1446 Da) and potassiated ($[M_1 + M_2 + K]^+$, theoretical mass of 633.1005 Da) heterodimer consisting of one dihydroxylated and one trihydroxylated flavan-3-ol unit were observed. A peak corresponding to the mass of a protonated heterodimer (theoretical mass of 621.1967 Da) containing one monohydroxydimethoxylated flavan-3-ol group and one trimethoxylated flavan-3-ol group was seen in the positive-ion mass spectra of all four red wine samples. That compound had not previously been reported in wine samples. A peak corresponding to another protonated heterodimer (theoretical mass of 637.1916 Da), containing two hydroxy and three methoxy constituents, was observed in the Corbiere spectrum—another previously unreported species in wine. The disposition of these groups within the molecular structure cannot be determined by mass measurement alone.

Flavonols and Flavanonols. Flavonols and flavanonols (see Figure 3) are members of the flavanoid family (*50*). These compounds were believed to exist only in the glucoside form in grapes. The present spectra show peaks corresponding to the masses of both glucosidic flavanonols and flavonols in wine. Peaks corresponding to potassiated 1-hydroxy flavanonol (taxifolin) glucoside ($[M + K]^+$, theoretical mass of 489.0794 Da) and 2-methoxy flavanonol glucoside (theoretical mass of 549.1006 Da) were found in all of the red wine mass spectra. A peak corresponding to potassiated 1-methoxy-2-hydroxy flavanonol glucoside (theoretical mass of 535.0849 Da) was identified in the Corbiere mass spectrum. Peaks corresponding to the potassiated 2-methoxy-1-hydroxy flavonol glucoside (theoretical mass of 547.0849 Da) were identified in all of the red wine samples. No flavanonols or flavonols were found in the white wine.

Cinnamic Acids and Coumarins. Grapes and wine contain cinnamic acids (see Figure 3) and their coumarin derivatives. Cinnamic acids are present in both red and white wines, forming the major phenolic component of the latter. Although these compounds themselves have no particular odor or flavor; they are precursors of volatile phenols that contribute to the organoleptic properties of the wine (*4*). Peaks corresponding to sodiated esculin (Figure 3, $[M + Na]^+$, theoretical mass of 363.0687 Da), glucosyl-*p*-caffeic acid (R3 = OH; R2, R5 = H; theoretical mass of 365.0844 Da), glucosyl-*p*-methoxy, hydroxy cinnamic acid (theoretical mass of 395.0950 Da), glucosyl-*p*-sinapic acid (R3, R5 = OCH_3; R2 = H; theoretical mass of 409.1106 Da), glucosyltrimethoxycinnamic acid (theoretical mass of 439.1212 Da), and potassiated glucosyl-*p*-coumaric acid (R2, R3, R5 = H; theoretical mass of 365.0634 Da) were observed in the spectra of all five of the wines. Peaks corresponding to sodiated glucosyl-*p*-ferulic acid (R3 = OCH_3; R2, R5 = H; theoretical mass of 379.09996 Da) were observed in the spectra of the Corbiere, California Red, and Beaujolais red wines. A peak corresponding to sodiated glucosyl-*p*-hydroxy dimethoxycinnamic acid (theoretical mass of 425.1055 Da) was observed in the spectra of both the Corbiere and Beaujolais wines.

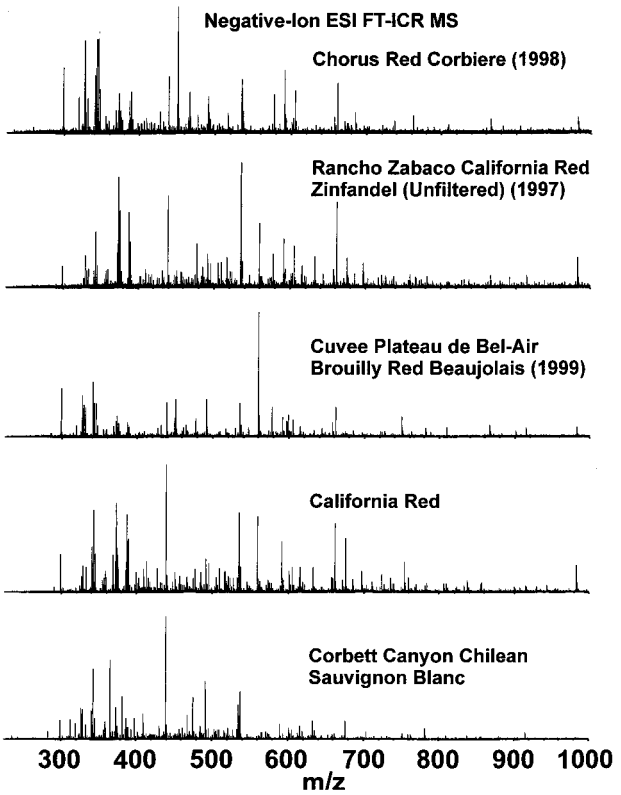

Figure 4. Negative-ion ESI FT-ICR mass spectrum of each of the same five wines as in Figure 1.

Carbohydrates. In addition to the phenolic compounds described above, a number of species having masses corresponding to those of carbohydrates were identified. It is particularly important to remember that mass alone cannot distinguish between optical isomers (as for carbohydrates). Peaks with mass corresponding to either potassiated arabinofuranosyl glucoside or apiofuranosyl glucopyranoside (theoretical mass of 351.0689 Da) were observed in all of the positive mode wine spectra. The base (i.e., largest) peak in the positive-ion mass spectrum of each of the five wines corresponds to potassiated sucrose (theoretical mass of 381.0794 Da). Peaks with mass corresponding to potassiated trisaccharides (theoretical mass of 543.1323 Da) and tetrasaccharides (theoretical mass of 705.1855 Da) were observed in all of the red wine positive-ion mass spectra, whereas Sauvignon Blanc showed the trisaccharide only. A peak corresponding to another potassiated oligosaccharide consisting of either two units of arabinofuranosyl glucoside or apiofuranosyl glucopyranoside (theoretical mass of 645.1639) was observed in the positive-ion mass spectra of all five wines.

Negative-Ion Electrospray. The negative-ion ($[M - H]^-$) ESI FT-ICR mass spectra obtained for the same five wines as in Figure 1 are shown in Figure 4. On the basis of internal calibration, the average root-mean-square error over the range $299 < m/z < 605$ is 0.26 ppm (i.e., about twice as accurate as for the positive-ion mass spectra). A mass scale expanded segment from 500 to 600 Da of the California Red spectrum (Figure 5) illustrates the spectral complexity. The inset in Figure 5 shows a further mass scale expansion, reveal-

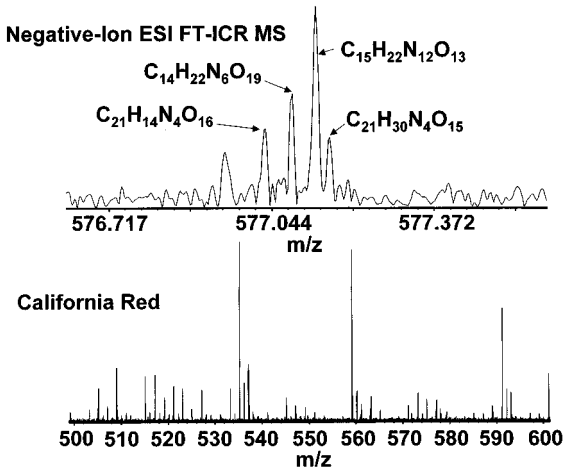

Figure 5. Mass scale-expanded segment ($500 < m/z < 600$) of the negative-ion ESI FT-ICR mass spectrum of California Red wine. (Inset) Further scale expansion for the region near m/z 577 Da, showing the resolution (and molecular formula assignments) of ions of different elemental composition at the same nominal mass.

ing the resolution and elemental composition assignments for several singly charged ions of the same nominal mass.

Elemental Compositions (Molecular Formulas). It was convenient to analyze the *positive*-ion ESI FT-ICR MS data by searching for different molecular classes of compounds previously identified in wine. However, the lower dynamic range and higher mass accuracy of the *negative*-ion ESI FT-ICR MS wine data make it feasible to assign unique elemental compositions without reference to prior information.

Each mass spectrum contained 100−200 peaks of abundance >5% of that of the highest peak. Tables 1−5 list the masses of the most abundant ions, along with neutral mass for each (obtained by adding the mass of a proton) and its assigned (neutral) elemental composition. The mass accuracy for each unique elemental assignment is shown. The number of possible elemental compositions increases as mass increases above ~450 Da. In some cases, it was not possible to assign a molecular formula, presumably due to the presence of an additional element in the compound. Scrutiny of Tables 1−5 reveals that although some compounds are common to some or all of the samples (albeit with some variation in relative abundances), other peaks are peculiar to a given wine. The variation in relative abundances is illustrated in Figure 6 for five of the identified compounds.

Elemental composition assignment was highly successful. Unique elemental compositions were achieved for 94% of the most abundant peaks in the Corbiere mass spectrum, compared to 76, 80, 76, and 85% for Zinfandel, Beaujolais, California Red, and Sauvignon Blanc wines, respectively. At lower mass, elemental compositions were limited to carbon, hydrogen, and oxygen. At higher mass, nitrogen incorporation was observed. Sulfur-containing compounds were observed in Sauvignon Blanc, California Red, and Zinfandel wines. From this point on, each listed elemental composition refers to the neutral molecule, not the deprotonated ion observed by mass spectrometry.

Corbiere. The Corbiere negative-ion mass spectrum contains ions of 347.0619, 467.0469, and 685.1255 Da at relative abundances of 35, 33, and 17%, respectively,

Table 1. Elemental Compositions Assigned to Peaks (>15% Relative Abundance) in the Negative-Ion ESI FT-ICR Mass Spectrum of Chorus Red Corbiere (1998) Wine[a]

ion mass	neutral mass	relative abundance	elemental composition(s)	
299.02563	300.03291	52	$C_8H_{12}O_{12}$	−0.11 ppm
319.03073	320.03801	29	$C_{11}H_{12}O_{11}$	−0.15 ppm
327.05682	328.0641	74	$C_{10}H_{16}O_{12}$	0.23 ppm
329.07248	330.07976	17	$C_{10}H_{18}O_{12}$	0.20 ppm
331.08819	332.09547	29	$C_{10}H_{20}O_{12}$	0.02 ppm
341.03613	342.04341	47	$C_{10}H_{14}O_{13}$	0.09 ppm
343.05162	344.0589	75	$C_{10}H_{16}O_{13}$	0.55 ppm
345.06751	346.07479	75	$C_{10}H_{18}O_{13}$	−0.14 ppm
347.06193	348.06921	35	$C_{13}H_{16}O_{11}$	0.15 ppm
369.06718	370.07446	19	$C_{12}H_{18}O_{13}$	0.76 ppm
371.08314	372.09042	19	$C_{12}H_{20}O_{13}$	−0.08 ppm
373.09879	374.10607	32	$C_{12}H_{22}O_{13}$	−0.08 ppm
375.11424	376.12152	18	$C_{12}H_{24}O_{13}$	0.45 ppm
387.07786	388.08514	26	$C_{12}H_{20}O_{14}$	0.43 ppm
389.09369	390.10097	33	$C_{12}H_{22}O_{14}$	−0.04 ppm
427.03415	428.04143	18	$C_9H_{12}N_6O_{14}$	−0.66 ppm
439.07639	440.08367	45	$C_{33}H_{12}O_2$	0.13 ppm
439.08518	440.09246	25	$C_{15}H_{16}N_6O_{10}$	0.75 ppm
451.05146	452.05874	100	$C_{19}H_{16}O_{13}$	0.77 ppm
452.05472	453.06200	19	$C_{18}{}^{13}CH_{16}O_{13}$	
467.04693	468.05421	33	$C_{19}H_{16}O_{14}$	−0.44 ppm
491.12597	492.13325	30	$C_{30}H_{16}N_6O_2$	0.45 ppm
517.14101	518.14829	16	$C_{18}H_{30}O_{17}$	0.02 ppm
535.15184	536.15912	43	$C_{18}H_{32}O_{18}$	−0.48 ppm
537.1667	538.17398	18	$C_{31}H_{26}N_2O_7$	0.04 ppm
577.13537	578.14265	31	$C_{15}H_{22}N_{12}O_{13}$	0.48 ppm
591.10255	592.10983	50	$C_{15}H_{24}N_6O_{19}$	−0.35 ppm
592.10554	593.11282	15	$C_{14}{}^{13}CH_{24}N_6O_{19}$	
605.19303	606.20031	34	$C_{22}H_{38}O_{19}$	0.70 ppm
661.18297	662.19025	40		
685.12552	686.1328	17	$C_{28}H_{30}O_{20}$, $C_{41}H_{22}N_2O_9$	

[a] All ions are singly charged and result from deprotonation of the parent neutral to yield $[M - H]^-$. Blank entries designate ions of unassigned elemental composition.

corresponding to compositions of $C_{13}H_{16}O_{11}$, $C_{19}H_{16}O_{14}$, and either $C_{28}H_{30}O_{20}$ or $C_{41}H_{22}N_2O_9$. In contrast, ions of 347.0619 Da (9% relative abundance) are observed in the Beaujolais spectrum but are not seen in the remaining three wines. It is interesting that those species are present in the French wines but are absent from the wines of U.S. and South American origin. Ions of 467.0469 Da are observed in the California Red and Zinfandel mass spectra but at much lower relative abundances, 7 and 8%, than for Corbiere. Ions of 685.1255 Da are also observed in the California Red and Zinfandel mass spectra, again at lower relative abundance (10% in each case) than for Corbiere. Finally, the most abundant ions in the Corbiere mass spectrum (451.0515 Da) correspond to the elemental composition $C_{19}H_{16}O_{13}$. Those ions are also observed in the California Red, Zinfandel, and Beaujolais spectra but at much lower relative abundances (16, 14, and 30%, respectively).

Red Zinfandel. The Zinfandel spectrum contained ions of 491.1053 Da ($C_{20}H_{20}N_4O_{11}$, $C_{12}H_{24}N_6O_{13}S$, or $C_{20}H_{28}O_{10}S_2$), 505.1410 Da (neutral composition, $C_{17}H_{30}O_{17}$), and 593.0298 Da ($C_{38}H_{10}O_8$) at relative abundances of 18, 20, and 16%, respectively. Ions of 491.1053 Da were also observed in the Beaujolais (10%), California Red (5%), and Sauvignon Blanc (5%) spectra. Ions of 505.1410 Da were also observed in the Corbiere (12%), California Red (8%), and Sauvignon Blanc (6%) spectra. A peak at 593.0298 Da was also observed in the California Red spectrum at a relative abundance of 10%. The base peak in the Zinfandel spectrum at 535.1521 Da corresponds to $C_{18}H_{32}O_{18}$. That peak appeared in the mass spectra of all of the wines at relative abundances

Table 2. Elemental Compositions Assigned to Peaks (>15% Relative Abundance) in the Negative-Ion ESI FT-ICR Mass Spectrum of Rancho Zabaco California Red Zinfandel (Unfiltered) (1997) Wine[a]

ion mass	neutral mass	relative abundance	elemental composition(s)	
299.02572	300.033	18	$C_8H_{12}O_{12}$	−0.41 ppm
329.07256	330.07984	26	$C_{10}H_{18}O_{12}$	−0.04 ppm
333.05935	334.06663	16	$C_{20}H_{14}O_3S$	−0.79 ppm
343.05164	344.05892	45	$C_{10}H_{16}O_{13}$	0.49 ppm
345.06763	346.07491	18	$C_{10}H_{18}O_{13}$	−0.49 ppm
359.11935	360.12663	15	$C_{12}H_{24}O_{12}$	0.40 ppm
371.0833	372.09058	28	$C_{12}H_{20}O_{13}$	−0.51 ppm
373.0987	374.10598	90	$C_{12}H_{22}O_{13}$	0.16 ppm
375.11436	376.12164	63	$C_{12}H_{24}O_{13}$	0.14 ppm
387.07795	388.08523	61	$C_{12}H_{20}O_{14}$	0.19 ppm
389.09362	390.1009	38	$C_{12}H_{22}O_{14}$	0.14 ppm
409.06588	410.07316	15	$C_{32}H_{10}O$	0.01 ppm
439.07662	440.0839	74	$C_{33}H_{12}O_2$	−0.39 ppm
439.08584	440.09312	67	$C_{15}H_{16}N_6O_{10}$	−0.75 ppm
477.06752	478.0748	36	$C_{21}H_{18}O_{13}$	−0.12 ppm
485.05518	486.06246	17	$C_{15}H_{14}N_6O_{13}$	−1.19 ppm
491.10528	492.11256	18	$C_{20}H_{20}N_4O_{11}$, $C_{12}H_{24}N_6O_{13}S$, $C_{20}H_{28}O_{10}S_2$	
491.12624	492.13352	28	$C_{30}H_{16}N_6O_2$, $C_{17}H_{24}N_4O_{13}$	
495.04332	496.0506	19	$C_{21}H_{12}N_4O_{11}$	−0.69 ppm
505.14102	506.1483	20	$C_{17}H_{30}O_{17}$	0.002 ppm
509.03104	510.03832	21	$C_{16}H_6N_{12}O_9$	−0.49 ppm
517.14159	518.14887	24	$C_{18}H_{30}O_{17}$	−1.10 ppm
535.1521	536.15938	100	$C_{18}H_{32}O_{18}$	0.96 ppm
536.15583	537.16311	22	$C_{17}{}^{13}CH_{32}O_{18}$	
537.06162	538.0689	21		
537.16655	538.17383	16	$C_{31}H_{26}N_2O_7$	0.31 ppm
559.11614	560.12342	52	$C_{19}H_{28}O_{19}$	−1.68 ppm
577.13625	578.14353	28	$C_{15}H_{22}N_{12}O_{13}$	1.00 ppm
591.10292	592.1102	10	$C_{15}H_{24}N_6O_{19}$	0.97 ppm
593.02981	594.03709	16	$C_{38}H_{10}O_8$	0.80 ppm
605.19292	606.2002	34	$C_{22}H_{38}O_{19}$	0.87 ppm
616.11014	617.11742	18	$C_{16}H_{19}N_{13}O_{14}$, $C_{31}H_{23}NO_{13}$	
633.12961	634.13689	25	$C_{22}H_{22}N_{10}O_{13}$	−0.17 ppm
657.0938	658.10108	15		
661.18414	662.19142	68		
675.10607	676.11335	24		
697.20381	698.21109	20		
983.27351	984.28079	24		

[a]Blank entries designate ions of unassigned elemental composition.

Table 3. Elemental Compositions Assigned to Peaks (>10% Relative Abundance) in the Negative-Ion ESI FT-ICR Mass Spectrum of Cuvee Plateau de Bel-Air, Brouilly Red Beaujolais (1999) Wine[a]

ion mass	neutral mass	relative abundance	elemental composition(s)	
299.02572	300.033	38	$C_8H_{12}O_{12}$	−0.41 ppm
327.05683	328.06411	32	$C_{10}H_{16}O_{12}$	0.20 ppm
329.07263	330.07991	26	$C_{10}H_{18}O_{12}$	−0.25 ppm
331.0884	332.09568	24	$C_{10}H_{20}O_{12}$	−0.61 ppm
341.03623	342.04351	44	$C_{10}H_{14}O_{13}$	−0.20 ppm
343.05165	344.05893	27	$C_{10}H_{16}O_{13}$	0.47 ppm
345.06758	346.07486	27	$C_{10}H_{18}O_{13}$	−0.35 ppm
371.08334	372.09062	13	$C_{12}H_{20}O_{13}$	−0.62 ppm
373.0987	374.10598	17	$C_{12}H_{22}O_{13}$	0.16 ppm
375.1143	376.12158	11	$C_{12}H_{24}O_{13}$	0.30 ppm
387.07784	388.08512	12	$C_{12}H_{20}O_{14}$	0.48 ppm
439.0766	440.08388	14	$C_{33}H_{12}O_2$	−0.34 ppm
439.08551	440.09279	27	$C_{15}H_{16}N_6O_{10}$	0.002 ppm
449.10886	450.11614	15	$C_{21}H_{22}O_{11}$	0.16 ppm
451.05138	452.05866	30	$C_{19}H_{16}O_{13}$	0.95 ppm
465.10402	466.1113	10	$C_{21}H_{22}O_{12}$	−0.37 ppm
477.06701	478.07429	15	$C_{21}H_{18}O_{13}$	0.94 ppm
491.12592	492.1332	30	$C_{30}H_{16}N_6O_2$, $C_{17}H_{24}N_4O_{15}$	
535.15175	536.15903	27	$C_{18}H_{32}O_{18}$	−0.31 ppm
559.11504	560.12232	100	$C_{19}H_{28}O_{19}$	0.28 ppm
560.1183	561.12558	18	$C_{18}{}^{13}CH_{28}O_{19}$	
577.13516	578.14244	24	$C_{15}H_{22}N_{12}O_{13}$	0.85 ppm
591.10212	592.1094	17	$C_{15}H_{24}N_6O_{19}$	0.38 ppm
591.17724	592.18452	11	$C_{21}H_{36}O_{19}$, $C_{34}H_{28}N_2O_8$	
597.07149	598.07877	13	$C_{21}H_{14}N_{10}O_{12}$	0.83 ppm
599.1251	600.13238	18	$C_{25}H_{28}O_{17}$, $C_{38}H_{20}N_2O_6$	
605.19292	606.2002	15	$C_{22}H_{38}O_{19}$	0.87 ppm
657.09189	658.09917	12		
661.1825	662.18978	24		
749.16324	750.17052	17	$C_{26}H_{38}O_{25}$, $C_{40}H_{26}N_6O_{10}$	

[a]Blank entries designate ions of unassigned elemental composition.

of >25%. Other major species in this spectrum included ions of 373.0987 Da ($C_{12}H_{22}O_{13}$) and 439.0766 Da ($C_{33}H_{12}O_2$). The peak at 373.0987 Da was also prominent in the California Red spectrum and appeared (at lower abundance) in all of the mass spectra. The peak at 439.0766 Da was also prominent for Zinfandel; it was the base peak for both Sauvignon Blanc and California Red but was present at much lower abundance for Beaujolais.

Beaujolais. The Beaujolais mass spectrum revealed ions of 449.1089 Da ($C_{21}H_{22}O_{11}$), 465.1040 Da ($C_{21}H_{22}O_{12}$), 591.1772 Da ($C_{21}H_{36}O_{19}$ or $C_{34}H_{28}N_2O_8$), 597.0715 Da ($C_{21}H_{14}N_{10}O_{12}$), 599.1251 Da ($C_{25}H_{28}O_{17}$ or $C_{38}H_{20}N_2O_6$), and 749.1632 Da ($C_{26}H_{38}O_{25}$ or $C_{40}H_{26}N_6O_{10}$) at relative abundances of >10%. A peak at 449.1089 Da also occurred in the Corbiere and Zinfandel mass spectra at 5 and 9% abundances. Ions of 465.1040, 591.1772, and 599.1251 Da were also observed for Zinfandel at abundances of 6, 8, and 6%. Ions of 597.0715 and 749.1632 Da were observed *only* for Beaujolais. The base peak in that spectrum, at 559.1150 Da, corresponds to $C_{19}H_{28}O_{19}$. That peak was also prominent for California Red (60%) and Zinfandel (52%) but was absent for the other wines.

California Red. The California Red mass spectrum showed ions of 399.1143 Da ($C_{14}H_{24}O_{13}$ or $C_{27}H_{16}N_2O_2$) and 753.1583 Da ($C_{25}H_{38}O_{26}$ or $C_{23}H_{26}N_{14}O_{16}$) that were not observed in any of the other mass spectra. It also contained a peak at 385.0623 Da ($C_{12}H_{18}O_{14}$, 17% abundance), also present in the Sauvignon Blanc, Corbiere, and Zinfandel mass spectra (8% abundance); a peak at 413.0938 Da ($C_{14}H_{22}O_{14}$ or $C_{20}H_{14}N_8OS$, 23% abundance), also seen in Corbiere (8% abundance); and a peak at 515.1249 Da ($C_{18}H_{28}O_{17}$, 16% abundance), also seen in Sauvignon Blanc (8% abundance). As mentioned above, the base peak in this spectrum, at 439.0766 Da, corresponds to $C_{33}H_{12}O_2$.

Sauvignon Blanc. The Sauvignon Blanc mass spectrum contained peaks at 313.0776 Da ($C_{10}H_{18}O_{11}$), 365.0124 Da ($C_{11}H_6N_6O_9$), 381.0073 Da ($C_{11}H_6N_6O_{10}$), 397.0022 Da ($C_{11}H_6N_6O_{11}$), 431.0263 Da ($C_{12}H_{12}N_6O_{10}S$ or $C_{20}H_{16}O_7S_2$), and 589.1015 Da ($C_{17}H_{10}N_{20}O_6$ or $C_{32}H_{14}N_8O_5$) that were not observed for any of the other wines. The peak at 365.0124 Da was prominent (62% abundance). The mass spectrum also exhibited ions of 341.1089 Da ($C_{12}H_{22}O_{11}$), 22% abundance), also seen in California Red (6%), Corbiere (7%), and Zinfandel (5%); ions of 467.1072 ($C_{19}H_{16}N_8O_7$, 19% abundance), also seen in California Red (8% abundance); and ions of 475.1303 Da ($C_{16}H_{28}O_{16}$, 33% abundance), also seen in the California Red and Zinfandel spectra (11 and 10%, respectively). The base peak in the Sauvignon Blanc mass spectrum, at 439.0766 Da, corresponds to $C_{33}H_{12}O_2$.

Electrospray Ionization Selectivity. Electrospray ionization efficiency can vary markedly for molecules of different acidity (negative-ion electrospray) or basicity (positive-ion electrospray), a point particularly pertinent to electrospray ionization of mixtures. In positive-ion ESI, a neutral typically adds a proton or alkali metal cation, so that the most basic molecules are typically most prominent in the ESI mass spectrum. Moreover,

Table 4. Elemental Compositions Assigned to Peaks (>15% Relative Abundance) in the Negative-Ion ESI FT-ICR Mass Spectrum of California Red Wine[a]

ion mass	neutral mass	relative abundance	elemental composition(s)	
299.02569	300.03297	29	$C_8H_{12}O_{12}$	−0.31 ppm
329.07269	330.07997	21	$C_{10}H_{18}O_{12}$	−0.44 ppm
333.05937	334.06665	19	$C_{20}H_{14}O_3S$	−0.85 ppm
341.03624	342.04352	35	$C_{10}H_{14}O_{13}$	−0.23 ppm
343.05168	344.05896	64	$C_{10}H_{16}O_{13}$	0.38 ppm
345.06761	346.07489	29	$C_{10}H_{18}O_{13}$	−0.43 ppm
359.11955	360.12683	17	$C_{12}H_{24}O_{12}$	−0.15 ppm
369.06726	370.07454	28	$C_{12}H_{18}O_{13}$	0.54 ppm
371.0834	372.09068	24	$C_{12}H_{20}O_{13}$	−0.78 ppm
373.09879	374.10607	68	$C_{12}H_{22}O_{13}$	−0.08 ppm
375.11434	376.12162	28	$C_{12}H_{24}O_{13}$	0.19 ppm
385.06232	386.0696	17	$C_{12}H_{18}O_{14}$	0.14 ppm
387.078	388.08528	60	$C_{12}H_{20}O_{14}$	0.06 ppm
389.09372	390.101	41	$C_{12}H_{22}O_{14}$	−0.12 ppm
399.11426	400.12154	16	$C_{14}H_{24}O_{13}$, $C_{27}H_{16}N_2O_2$	
409.06589	410.07317	17	$C_{32}H_{10}O$	−0.01 ppm
413.09377	414.10105	23	$C_{14}H_{22}O_{14}$, $C_{20}H_{14}N_8OS$	
427.03436	428.04164	18	$C_9H_{12}N_6O_{14}$	−1.15 ppm
439.07659	440.08387	100	$C_{33}H_{12}O_2$	−0.32 ppm
439.08582	440.0931	39	$C_{15}H_{16}N_6O_{10}$	−0.70 ppm
451.05142	452.0587	16	$C_{19}H_{16}O_{13}$	0.86 ppm
477.06759	478.07487	18	$C_{21}H_{18}O_{13}$	−0.27 ppm
485.05482	486.0621	16	$C_{15}H_{14}N_6O_{13}$	−0.44 ppm
491.12607	492.13335	25	$C_{30}H_{16}N_6O_2$, $C_{17}H_{24}N_4O_{13}$	
495.04327	496.05055	22	$C_{21}H_{12}N_4O_{11}$	−0.59 ppm
509.02217	510.02945	18	$C_{21}H_{10}N_4O_{12}$	0.14 ppm
515.12494	516.13222	16	$C_{18}H_{28}O_{17}$	0.83 ppm
517.14136	518.14864	17	$C_{18}H_{30}O_{17}$	−0.66 ppm
535.15196	536.15924	61	$C_{18}H_{32}O_{18}$	−0.70 ppm
537.0538	538.06108	19		
559.11584	560.12312	59	$C_{19}H_{28}O_{19}$	−1.14 ppm
591.10264	592.10992	39	$C_{15}H_{24}N_6O_{19}$	−0.50 ppm
601.12902	602.1363	16	$C_{23}H_{22}N_8O_{12}$	−0.97 ppm
605.19291	606.20019	19	$C_{22}H_{38}O_{19}$	0.89 ppm
616.10965	617.11693	19	$C_{16}H_{19}N_{13}O_{14}$, $C_{31}H_{23}NO_{13}$	
633.12946	634.13674	19	$C_{22}H_{22}N_{10}O_{13}$	0.06 ppm
661.18385	662.19113	53		
675.10706	676.11434	41		
697.2036	698.21088	16		
753.15832	754.1656	23	$C_{25}H_{38}O_{26}$, $C_{23}H_{26}N_{14}O_{16}$	
983.2727	984.27998	20		

[a] Blank entries designate ions of unassigned elemental composition.

in a mixture of molecules, lower basicity species that might be observed if present alone may be "suppressed" in a mixture containing species of higher acidity (*51*). Conversely, in negative-ion ESI, a neutral typically loses a proton, so that the most acidic molecules are typically most efficiently ionized. The relatively high dynamic range of our instrument can offset somewhat such differences in ionization efficiency, but it is important to recognize that the relative abundances of electrosprayed ions do not in general accurately reflect the relative abundances of their precursor neutrals in the original solution. For example, we see virtually no peaks below *m*/*z* 300, even though several species in that range are readily detected as volatiles by GC-MS—evidently the higher mass components in wine are more efficiently ionized by electrospray than the lower mass components. Despite electrospray ionization efficiency differences, we are still able to resolve 100−200 different molecular formulas in a single negative-ion ESI FT-ICR mass spectra of wine, with marked differences between different wines. Thus, it seems reasonable to project the possible use of such mass spectra as a "fingerprint" for discriminating between different wines.

Mass Resolution. For simplicity and speed, all experiments were performed by exciting and detecting ions over a broad mass range. However, it is possible to achieve much higher mass resolution over a narrower mass range in several ways. For example, in the current experiments, ions were transferred from the electrospray source via a system of multipoles including a quadrupole operated in radio frequency-only mode. However, the quadrupole could be operated such that ions of only selected *m*/*z* values are transferred to the FT-ICR cell, thereby increasing both mass resolution and dynamic range (*52*). Moreover, stored-waveform inverse Fourier transform (SWIFT) mass selection ion ejection (*53*−*55*) and/or analogue (*29*) or digital (*56*) heterodyne detection can significantly increase mass resolution. Finally, as will be reported in future investigations, once an ion of interest has been identified on the basis of its accurate mass (and thus its chemical formula), additional tandem (MS/MS) techniques can help to elucidate the molecular structure.

Table 5. Elemental Compositions Assigned to Peaks (>10% Relative Abundance) in the Negative-Ion ESI FT-ICR Mass Spectrum of Corbett Canyon Chilean Sauvignon Blanc Wine[a]

ion mass	neutral mass	relative abundance	elemental composition(s)	
299.0256	300.03288	16	$C_8H_{12}O_{12}$	−0.01 ppm
313.07762	314.0849	17	$C_{10}H_{18}O_{11}$	0.04 ppm
319.03396	320.04124	13		
327.05685	328.06413	25	$C_{10}H_{16}O_{12}$	0.14 ppm
329.0725	330.07978	24	$C_{10}H_{18}O_{12}$	0.14 ppm
333.05917	334.06645	12	$C_{20}H_{14}O_3S$	−0.25 ppm
341.0361	342.04338	23	$C_{10}H_{14}O_{13}$	0.18 ppm
341.10887	342.11615	22	$C_{12}H_{22}O_{11}$	0.18 ppm
343.05176	344.05904	56	$C_{10}H_{16}O_{13}$	0.15 ppm
345.06739	346.07467	17	$C_{10}H_{18}O_{13}$	0.20 ppm
359.11943	360.12671	15	$C_{12}H_{24}O_{12}$	0.18 ppm
365.0124	366.01968	62	$C_{11}H_6N_6O_9$	−0.15 ppm
373.09867	374.10595	25	$C_{12}H_{22}O_{13}$	0.24 ppm
375.11442	376.1217	11	$C_{12}H_{24}O_{13}$	−0.02 ppm
381.00732	382.0146	34	$C_{11}H_6N_6O_{10}$	−0.16 ppm
387.07797	388.08525	17	$C_{12}H_{20}O_{14}$	0.14 ppm
389.09352	390.1008	10	$C_{12}H_{22}O_{14}$	0.40 ppm
397.00218	398.00946	17	$C_{11}H_6N_6O_{11}$	−0.01 ppm
409.06555	410.07283	20	$C_{32}H_{10}O$	0.82 ppm
431.02632	432.0336	11	$C_{12}H_{12}N_6O_{10}S_1$, $C_{20}H_{16}O_7S_2$	
439.0761	440.08338	100	$C_{33}H_{12}O_2$	0.79 ppm
439.08525	440.09253	27	$C_{15}H_{16}N_6O_{10}$	0.59 ppm
440.07949	441.08677	12	$C_{32}{}^{13}CH_{12}O_2$	
467.10721	468.11449	19	$C_{19}H_{16}N_8O_7$	−0.63 ppm
475.13031	476.13759	33	$C_{16}H_{28}O_{16}$	0.30 ppm
485.05458	486.06186	11	$C_{15}H_{14}N_6O_{13}$	0.05 ppm
491.12505	492.13233	47	$C_{29}H_{20}N_2O_6$, $C_{16}H_{28}O_{17}$	
535.15135	536.15863	28	$C_{18}H_{32}O_{18}$	0.44 ppm
537.05291	538.06019	38		
589.10154	590.10882	12	$C_{32}H_{14}N_8O_5$, $C_{19}H_{22}N_6O_{16}$	
601.12866	602.13594	10		
616.10862	617.1159	11	$C_{16}H_{19}N_{13}O_{14}$, $C_{31}H_{23}NO_{13}$	
675.10516	676.11244	15		

[a] Blank entries designate ions of unassigned elemental composition.

Conclusion. The high resolution and mass accuracy of Fourier transform ion cyclotron mass spectrometry make it nonpareil for single-stage analysis of complex mixtures such as wine. For example, >30 (mostly previously known) compounds were identified in the positive-ion ESI FT-ICR mass spectra, without any prior separation or purification. The positive-ion mass spectra were dominated by potassiated sucrose and (for the red wines) anthocyanins. The negative-ion ESI FT-ICR mass spectra showed far greater variation among different wines, with respect to different components as well as different relative abundances of common components.

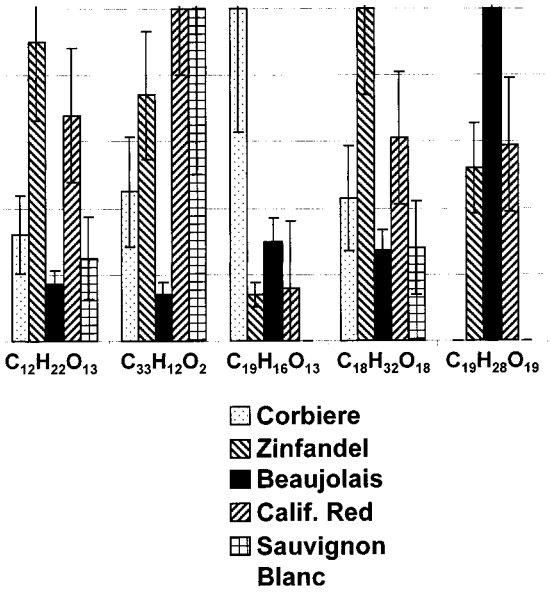

Figure 6. Variation in relative abundances of $C_{12}H_{22}O_{13}$, $C_{33}H_{12}O_2$, $C_{19}H_{16}O_{13}$, $C_{18}H_{32}O_{18}$, and $C_{19}H_{28}O_{19}$ in the negative-ESI mass spectra of Corbiere, Zinfandel, Beaujolais, California Red, and Sauvignon Blanc wines.

For classification of wines by ESI FT-ICR mass spectrometry, negative ions appear to be preferable to positive ions for two reasons. First, because negative ions are formed primarily by deprotonation, whereas positive ions may arise from attachment of any of several cations, inherently fewer elemental combinations exist. Second, because of the dominant sucrose $[M + K]^+$ peak, the mass spectral dynamic range is much more limited for positive ions than for negative ions. Unique elemental compositions could be assigned to 76−94% of negative ions of >10% relative abundance.

In summary, we believe that the lack of separation and purification requirements constitutes a significant advantage for wine analysis. Given the distinctive differences between negative-ion ESI mass spectra of different wines, it may be possible to classify wines on the basis of the mass spectral components that differ in presence and/or relative abundance. Further work is in progress to characterize variations among different monovarietal wines, wines of the same variety but different age, and different bottles or barrels from the same vintage.

LITERATURE CITED

(1) Markakis, P. *Anthocyanins as Food Colors*; Academic Press: New York, 1982.
(2) Lea, A. G. H.; Arnold, G. M. *J. Sci. Food Agric.* **1978**, *29*, 478−483.
(3) Mestres, M.; Busto, O.; Guasch, J. *J. Chromatogr. A* **2000**, *881*, 569−581.
(4) Ribereau-Gayon, P.; Glories, Y.; Maujean, A.; Dubourdieu, D. *Handbook of Enology*; Wiley: Chichester, U.K., 2000; Vol. 2.
(5) Lee, H. S.; Hong, V. *J. Chromatogr.* **1992**, *624*, 221−234.
(6) Kraemer-Schafhalter, A.; Fuchs, H.; Pfannhauser, W. *J. Sci. Food Agric.* **1998**, *78*, 435−440.
(7) da Costa, C. T.; Horton, D.; Margolis, S. A. *J. Chromatogr. A* **2000**, *881*, 403−410.
(8) Dallas, C.; Ricardo da Silva, J. M.; Laureano, O. *J. Agric. Food Chem.* **1996**, *44*, 2402−2407.
(9) Hong, V.; Wrolstad, R. E. *J. Agric. Food Chem.* **1990**, *38*, 708−715.
(10) Goiffon, J. P.; Brun, M.; Bourrier, M. J. *J. Chromatogr.* **1991**, *537*, 101−121.
(11) Williams, M.; Hradzina, G. *J. Chromatogr.* **1978**, *15*, 389−398.
(12) Glassgen, W. E.; Seitz, H. U.; Metzger, J. W. *Biol. Mass Spectrom.* **1992**, *21*, 271−277.
(13) Fenn, J. B.; Mann, M.; Meng, C. K.; Wong, S. F.; Whitehouse, C. M. *Science* **1989**, *246*, 64−71.
(14) Smith, R. D.; Loo, J. A.; Ogorzalek Loo, R. R.; Busman, M.; Udseth, H. R. *Mass Spectrom. Rev.* **1991**, *10*, 359−451.
(15) Hendrickson, C. L.; Emmett, M. R. *Annu. Rev. Phys. Chem.* **1999**, *50*, 517−536.
(16) Baldi, A.; Romani, A.; Mulinacci, N.; Vincieri, F. F.; Casetta, B. *J. Agric. Food Chem.* **1995**, *43*, 2104−2109.
(17) Favretto, D.; Flamini, R. *Am. J. Enol. Vitic.* **2000**, *51*, 55−64.
(18) Fulcrand, H.; Benabdeljalil, C.; Rigaud, J.; Cheynier, V.; Moutonet, M. *Phytochemistry* **1998**, *47*, 1401−1407.
(19) Perez-Margarino, S.; Revilla, I.; Gonzales-SanJose, M. L.; Beltran, S. *J. Chromatogr. A* **1999**, *847*, 75−81.
(20) Revilla, I.; Perez-Margarino, S.; Gonzales-SanJose, M. L.; Beltran, S. *J. Chromatogr. A* **1999**, *847*, 83−90.
(21) Wang, J.; Sporns, P. *J. Agric. Food Chem.* **1999**, *47*, 2009−2015.
(22) Edelmann, A.; Diewok, J.; Schuster, K. C.; Lendl, B. *J. Agric. Food Chem.* **2001**, *49*, 1139−1145.
(23) Siret, R.; Boursiquot, J. M.; Merle, M. H.; Cabanis, J. C.; This, P. *J. Agric. Food Chem.* **2000**, *48*, 5035−5040.
(24) Desportes, C.; Charpentier, M.; Duteutre, B.; Maujean, A.; Duchiron, F. *J. Chromatogr. A* **2000**, *893*, 281−291.
(25) Moreno-Arribas, M. V.; Bartolome, B.; Pueyo, E.; Polo, M. C. *J. Agric. Food Chem.* **1998**, *46*, 3422−3425.
(26) Aussenac, J.; Chassagne, D.; Claparols, C.; Charpentier, M.; Duteutre, B.; Feuillat, M.; Charpentier, C. *J. Chromatogr. A* **2001**, *907*, 155−164.
(27) Roggero, J. P.; Archier, P.; Coen, S. *Wine* **1997**, *661*, 6−11.
(28) Comisarow, M. B.; Marshall, A. G. *Chem. Phys. Lett.* **1974**, *25*, 282−283.
(29) Marshall, A. G.; Hendrickson, C. L.; Jackson, G. S. *Mass Spectrom. Rev.* **1998**, *17*, 1−35.
(30) Qian, K.; Rodgers, R. P.; Hendrickson, C. L.; Emmett, M. R.; Marshall, A. G. *Energy Fuels* **2001**, *15*, 492−498.
(31) Qian, K.; Robbins, W. K.; Hughey, C. A.; Cooper, H. J.; Rodgers, R. P.; Marshall, A. G. *Energy Fuels* **2001**, in press.
(32) Senko, M. W.; Hendrickson, C. L.; Pasa-Tolic, L.; Marto, J. A.; White, F. M.; Guan, S.; Marshall, A. G. *Rapid Commun. Mass Spectrom.* **1996**, *10*, 1824−1828.
(33) Senko, M. W.; Hendrickson, C. L.; Emmett, M. R.; Shi, S. D.-H.; Marshall, A. G. *J. Am. Soc. Mass Spectrom.* **1997**, *8*, 970−976.
(34) Marshall, A. G.; Guan, S. *Rapid Commun. Mass Spectrom.* **1996**, *10*, 1819−1823.
(35) Quinn, J. P.; Emmett, M. R.; Marshall, A. G. *46th ASMS Conference on Mass Spectrometry and Allied Topics*, Orlando, FL; American Society for Mass Spectrometry: Santa Fe, NM, 1998; pp 1388−1388.
(36) Chowdhury, S. K.; Katta, V.; Chait, B. T. *Rapid Commun. Mass Spectrom.* **1990**, *4*, 81−87.
(37) Beu, S. C.; Laude, D. A., Jr. *Int. J. Mass Spectrom. Ion Processes* **1992**, *112*, 215−230.
(38) Senko, M. W.; Canterbury, J. D.; Guan, S.; Marshall, A. G. *Rapid Commun. Mass Spectrom.* **1996**, *10*, 1839−1844.
(39) Ledford, E. B., Jr.; Rempel, D. L.; Gross, M. L. *Anal. Chem.* **1984**, *56*, 2744−2748.
(40) Shi, S. D.-H.; Drader, J. J.; Freitas, M. A.; Hendrickson, C. L.; Marshall, A. G. *Int. J. Mass Spectrom.* **2000**, *195/196*, 591−598.

(41) Blakney, G. T.; van der Rest, G.; Johnson, J. R.; Freitas, M. A.; Drader, J. J.; Shi, S. D.-H.; Hendrickson, C. L.; Kelleher, N. L.; Marshall, A. G. *Proceedings of the 49th American Society of Mass Spectrometry Conference on Mass Spectrometry and Allied Topics*, Chicago, IL; ASMS: Santa Fe, NM, 2001; WPM265.
(42) McLafferty, F. W.; Turecek, F. *Interpretation of Mass Spectra*; University Science Books: Sausalito, CA, 1993.
(43) Woodlin, R. L.; Bomse, D. S.; Beauchamp, J. L. *J. Am. Chem. Soc.* **1978**, *100*, 3248−3250.
(44) Little, D. P.; Speir, J. P.; Senko, M. W.; O'Connor, P. B.; McLafferty, F. W. *Anal. Chem.* **1994**, *66*, 2809−2815.
(45) Gauthier, J. W.; Trautman, T. R.; Jacobson, D. B. *Anal. Chim. Acta* **1991**, *246*, 211−225.
(46) Zubarev, R. A.; Kelleher, N. L.; McLafferty, F. W. *J. Am. Chem. Soc.* **1998**, *120*, 3265−3266.
(47) de Pascual-Teresa, S.; Rivas-Gonzalo, J. C.; Santos-Buelga, C. *Int. J. Food Sci. Technol.* **2000**, *35*, 33−40.
(48) Lazarus, S. A.; Adamson, G. E.; Hammerstone, J. F.; Schmitz, H. H. *J. Agric. Food Chem.* **1999**, *47*, 3693−3701.
(49) Fulcrand, H.; Remy, S.; Souquet, J.-M.; Cheynier, V. M. *J. Agric. Food Chem.* **1999**, *47*, 1023−1028.
(50) Cook, N. C.; Samman, S. *Nutr. Biochem.* **1996**, *7*, 66−76.
(51) Mann, M. *Org. Mass Spectrom.* **1990**, *25*, 575−587.
(52) Hendrickson, C. L.; Quinn, J. P.; Emmett, M. R.; Marshall, A. G. *Proceedings of the 49th American Society of Mass Spectrometry Annual Conference on Mass Spectrometry and Allied Topics*, Chicago, IL; ASMS: Santa Fe, NM, 2001; p MOC10:55.
(53) Marshall, A. G.; Wang, T.-C. L.; Ricca, T. L. *J. Am. Chem. Soc.* **1985**, *107*, 7893−7897.
(54) Wang, T.-C. L.; Ricca, T. L.; Marshall, A. G. *Anal. Chem.* **1986**, *58*, 2935−2938.
(55) Guan, S.; Marshall, A. G. *Int. J. Mass Spectrom. Ion Processes* **1996**, *157/158*, 5−37.
(56) Drader, J. J.; Shi, S. D.-H.; Blakney, G. T.; Hendrickson, C. L.; Laude, D. A.; Marshall, A. G. *Anal. Chem.* **1999**, *71*, 4758−4763.

Received for review July 3, 2001. Revised manuscript received September 22, 2001. Accepted September 22, 2001. This work was supported by the NSF National High-Field FT-ICR Mass Spectrometry Facility (CHE 99-09502), Florida State University, and the National High Magnetic Field Laboratory at Tallahassee, Florida.

JF0108516